[10] Li Y, Wu Y, Sakaguchi S, et al. Presence of regulatory T cells within tolerant graft of human liver and intestinal transplantation. Am J Transplant 2006;6 (12):1056.

[11] Parker CM, Groh V, Band H, et al. Evidence for extrathymic changes in the T cell receptor gamma/delta repertoire. J Exp Med 1990;171 (5):1597–612.

[12] Barakonyi A, Kovacs KT, Miko E, et al. Recognition of nonclassical HLA class I antigens by gamma delta T cells during pregnancy. J Immunol 2002;168(6):2683–8.

[13] Nagaeva O, Jonsson L, Mincheva-Nilsson L. Dominant IL-10 and TGF-beta mRNA expression in gammadelta T cells of human early pregnancy decidua suggests immunoregulatory potential. Am J Reprod Immunol 2002;48(1):9–17.

[14] Yoshitomi M, Koshiba T, Sakashita H, et al. Requirement of protocol biopsy before and after complete cessation of immunosuppression following living-donor liver transplantation. Am J Transplant 2006;6 (12):173.

Science
AAAS

Emerging Challenges in Regulatory T Cell Function and Biology

Shimon Sakaguchi, *et al.*

Science **317**, 627 (2007);
DOI: 10.1126/science.1142331

Science (print ISSN 0036-8075; online ISSN 1095-9203) is published weekly, except the last week in December, by the American Association for the Advancement of Science, 1200 New York Avenue NW, Washington, DC 20005.

Several cell-biological questions are of interest concerning these receptors: (i) Are they internalized, and where do they deliver bound antigens? (ii) Are some receptors better at programming cross-presentation? (iii) Can individual receptors target functionally distinct DC subpopulations? (iv) Does antibody binding to a given receptor trigger DC maturation, and if so, does receptor activation help to control the balance between immunity and tolerance? In general, we must ask what the relationship is between the mode of antigen endocytosis and the function of antigen presentation to T cells (Fig. 1).

In recent work published in *Science*, Dudziak *et al.* have shown that two lectin receptors on mouse DCs, DEC-205 and DCIR (33D1), are differentially expressed by two different populations of DCs in the spleen: $CD8\alpha^+$ and $CD8\alpha^-$ DCs, respectively (*22*). Targeting antigens via DEC-205 to the $CD8\alpha^+$ subset was found to selectively prime MHCI-restricted responses by cross-presentation, whereas MHCII-restricted responses were more efficiently triggered by DCIR targeting to the $CD8\alpha^-$ subset. This finding is consistent with the idea that cross-presentation is, in general, more the purview of $CD8\alpha^+$ DCs (*23*). Reversing cell-type restriction of receptor expression did not appear to change this conclusion substantially, suggesting that specializations associated with $CD8\alpha^+$ DCs may favor their ability for cross-presentation.

At the same time, in vitro work suggested that another lectin (the mannose receptor) was also quite effective at inducing the formation of peptide-MHCI complexes from exogenous antigen in bone marrow cultures and macrophages, where subpopulation identities are less clear (*24*). The mannose receptor appeared to deliver bound antibody to early endocytic compartments, suggesting that cross-presentation may occur from here as opposed to in late endosomes and lysosomes, which was the case for loading onto MHCII. Although these results suggest that the receptor used and route of antigen entry may also help determine the resulting form of antigen presentation, the data relied only on low-resolution qualitative immunofluorescence to define the intracellular localization of delivered antigens—criteria too limited to support a firm conclusion. Moreover, the data did not account for the fact that DEC-205, which also efficiently mediates MHCI-restricted cross-presentation, has been extensively characterized as delivering its bound antigens to late endosomes and lysosomes as opposed to early compartments (*25*). In any event, these findings highlight a whole new problem set involving the relative contributions of endocytosis and DC subpopulations in determining the nature of the immune response.

Looking Forward by Looking Backward

There are many other problems that would benefit immediately from a more effective and bidirectional relationship between immunologists and cell biologists. For example, the dynamics and function of the immunological synapse remain incompletely understood, in part because these critically important structures have yet to be subjected to the type of rigorous analysis applied to "simpler" problems of cell adhesion. The relationship between autophagy and antigen presentation in viral immunity is also emerging as critical (*26*, *27*). Signaling in immune cells will provide a rich area to mine, and some direct interchange over what lipid rafts can and cannot do would be of great value in itself. Finally, there is the issue that immunologists have always appreciated far better than most molecular cell biologists: the in vivo or systems-level context. Immunology exists to study the way the immune system works as a whole to confer protection against disease. Broad and conceptually profound, it is understandably difficult for the field to devote equivalent attention to the cellular mechanisms involved. However, further progress will require such effort, and the best path forward will be to take steps to make the language, concepts, and culture of immunology more accessible to colleagues in cell biology to attract them in and to outsource what may be too diversionary to learn. One area that is particularly ripe for spectacular advance is in the area of in vivo or "intravital" imaging. Although still in a largely descriptive phase of development, immunologists are nicely demonstrating to cell biologists the conceptual value of this platform. When this area is combined with emerging technologies to permit interventional experiments using actuation switches and quantitative molecular reporters, we will have entered a new age of "systems cell biology," combining the best of both worlds.

Like Elyot and Amanda, immunology and cell biology were once intimate partners; we find ourselves again in close proximity, but this time with the chance to rekindle a beautiful relationship.

References

1. J. C. Stinchcombe, E. Majorovits, G. Bossi, S. Fuller, G. M. Griffiths, *Nature* **443**, 462 (2006).
2. J. Stinchcombe, G. Bossi, G. M. Griffiths, *Science* **305**, 55 (2004).
3. D. B. Stetson *et al.*, *J. Exp. Med.* **198**, 1069 (2003).
4. P. R. Wolf, H. L. Ploegh, *Annu. Rev. Cell Dev. Biol.* **11**, 267 (1995).
5. P. Cresswell, *Annu. Rev. Immunol.* **12**, 259 (1994).
6. P. J. Peters, J. J. Neefjes, V. Oorschot, H. L. Ploegh, H. J. Geuze, *Nature* **349**, 669 (1991).
7. P. Pierre *et al.*, *Immunity* **4**, 229 (1996).
8. M. J. Kleijmeer, S. Morkowski, J. M. Griffith, A. Y. Rudensky, H. J. Geuze, *J. Cell Biol.* **139**, 639 (1997).
9. I. Mellman, R. M. Steinman, *Cell* **106**, 255 (2001).
10. S. Amigorena, J. R. Drake, P. Webster, I. Mellman, *Nature* **369**, 113 (1994).
11. E. S. Trombetta, I. Mellman, *Annu. Rev. Immunol.* **23**, 975 (2005).
12. A. R. Townsend, J. J. Skehel, *J. Exp. Med.* **160**, 552 (1984).
13. M. T. Heemels, H. Ploegh, *Annu. Rev. Biochem.* **64**, 463 (1995).
14. M. W. Moore, F. R. Carbone, M. J. Bevan, *Cell* **54**, 777 (1988).
15. L. Shen, L. J. Sigal, M. Boes, K. L. Rock, *Immunity* **21**, 155 (2004).
16. A. Rodriguez, A. Regnault, M. Kleijmeer, P. Ricciardi-Castagnoli, S. Amigorena, *Nat. Cell Biol.* **1**, 362 (1999).
17. A. Y. C. Huang, A. T. Bruce, D. M. Pardoll, H. I. Levitsky, *Immunity* **4**, 349 (1996).
18. N. Touret *et al.*, *Cell* **123**, 157 (2005).
19. A. L. Ackerman, A. Giodini, P. Cresswell, *Immunity* **25**, 607 (2006).
20. J. M. Lord, L. M. Roberts, *J. Cell Biol.* **140**, 733 (1998).
21. L. Bonifaz *et al.*, *J. Exp. Med.* **196**, 1627 (2002).
22. D. Dudziak *et al.*, *Science* **315**, 107 (2007).
23. P. Schnorrer *et al.*, *Proc. Natl. Acad. Sci. U.S.A.* **103**, 10729 (2006).
24. S. Burgdorf, A. Kautz, V. Böhnert, P. A. Knolle, C. Kurts, *Science* **316**, 612 (2007).
25. K. Mahnke *et al.*, *J. Cell Biol.* **151**, 673 (2000).
26. H. K. Lee, J. M. Lund, B. Ramanathan, N. Mizushima, A. Iwasaki, *Science* **315**, 1398 (2007).
27. D. Schmid, M. Pypaert, C. Munz, *Immunity* **26**, 79 (2007).

10.1126/science.1142955

PERSPECTIVE

Emerging Challenges in Regulatory T Cell Function and Biology

Shimon Sakaguchi[1] and Fiona Powrie[2]

Much progress has been made in understanding how the immune system is regulated, with a great deal of recent interest in naturally occurring $CD4^+$ regulatory T cells that actively engage in the maintenance of immunological self-tolerance and immune homeostasis. The challenge ahead for immunologists is the further elucidation of the molecular and cellular processes that govern the development and function of these cells. From this, exciting possibilities are emerging for the manipulation of regulatory T cell pathways in treating immunological diseases and suppressing or augmenting physiological immune responses.

Walter B. Cannon, the originator of the concept of homeostasis, emphasized in his book *The Wisdom of the Body* that "when a factor is known which can shift a homeostatic state in one direction it is reasonable to look for a factor or factors having an opposing

effect." The immune system is not an exception to this. It harbors not only effector lymphocytes capable of attacking invading microbes but also an inhibitory population of T cells, called regulatory T (T_{reg}) cells. These lymphocytes are specialized in suppressing excessive or misguided immune responses that can be harmful to the host; for example, against normal self-constituents in autoimmune disease, innocuous environmental substances in allergy, or commensal microbes in certain inflammatory diseases (*1*, *2*). On the other hand, overzealous T_{reg} responses can impede host protective immunity in infectious disease and cancer. Recent advances in our understanding of the molecular mechanisms that control T_{reg} cell development have opened new avenues of investigation, but key questions concerning the antigen specificity of T_{reg} cells, their homeostasis, and mechanism of action remain. Here we discuss our current understanding of the biology and function of T_{reg} cells and how they might be clinically exploited to control physiological and pathological immune responses to self- and nonself-antigens.

Naturally occurring $CD4^+$ T_{reg} cells, which constitute approximately 10% of peripheral $CD4^+$ T cells in normal individuals, characteristically express CD25 [the interleukin-2 (IL-2) receptor α chain, which is a component of the high-affinity IL-2 receptor] (*1*, *2*). $CD4^+CD25^+$ T_{reg} cells play a nonredundant role in maintaining immunological self-tolerance and immune homeostasis. Their importance is made evident by the fact that the depletion of this population from normal rodents produces a variety of autoimmune inflammatory diseases, whereas reconstitution with $CD4^+$ $CD25^+$ T cells can inhibit disease development (*1*, *2*). They are produced by the normal thymus as a functionally distinct and mature population, although there is evidence that T cells with similar immune suppressive activity can be generated from naïve T cells in the periphery.

The identification of the transcription factor forkhead box p3 (Foxp3) as being specifically expressed by T_{reg} cells and crucial for their function has provided a molecular framework for dissecting T_{reg} function (*3*–*5*) (Fig. 1). Mutations in the gene encoding Foxp3 in humans and mice result in impaired development and function of $CD4^+CD25^+$ natural T_{reg} cells and lead to autoimmune inflammatory pathology. This is best exemplified by a human genetic disease called IPEX (immune dysregulation, polyendocrinopathy, enteropathy, X-linked) syndrome, which is characterized by autoimmune disease (including type 1 diabetes and thyroiditis), allergy, and inflammatory bowel disease (IBD) (*6*). Further evidence for Foxp3 as a key controller of the development and suppressive function of natural T_{reg} cells comes from experiments in which transduction of the gene is sufficient to convert naïve T cells into T_{reg}-like cells (*3*–*5*). Notably, Foxp3 inhibits transcription of the gene encoding IL-2 and up-regulates the expression of CD25 and other T_{reg} cell–associated molecules (*3*, *4*). The resulting inability of $Foxp3^+$ T_{reg} cells to produce IL-2 appears to make them highly dependent on exogenous IL-2 for survival (*7*–*9*). Accordingly, mice genetically deficient in IL-2, CD25, or CD122 (the IL-2 receptor β chain) and humans with genetic deficiency of CD25 have both reduced numbers and impaired function of $Foxp3^+$ T_{reg} cells and succumb to severe autoimmune inflammatory disease (*8*, *10*).

A key question that has emerged from these findings is how Foxp3 orchestrates the cellular and molecular programs involved in T_{reg} function. Recent studies have shown that Foxp3 binds to other transcription factors such as NFAT (nuclear factor of activated T cells) and AML1 (acute leukemia-1)/Runx1 (runt-related transcription factor 1) and potentially interacts with activator protein 1 and nuclear factor κB (*11*–*13*). It is this Foxp3/NFAT/Runx1 complex, together with other coactivator or corepressor proteins, that is responsible for the observed repression of the IL-2 and other cytokine genes, as well as the activation of the genes for CD25, cytotoxic lymphocyte–associated antigen-4 (CTLA-4), and glucocorticoid-induced TNF receptor family–related protein (GITR) by binding to their respective promoters (*11*, *12*). MicroRNA genes also appear to be important in T_{reg} cell development; for example, T cell–specific depletion of Dicer, a ribonuclease enzyme required for processing double-stranded RNA, hampers thymic development of $Foxp3^+$ T cells and elicits IBD (*14*). In addition, it has been shown by genome-wide analysis combining chromatin immunoprecipitation with mouse genome tiling array profiling that Foxp3 directly or indirectly controls hundreds of genes, which include those that encode nuclear factors controlling gene expression and chromatin remodeling, membrane proteins, and signal transduction molecules (*15*, *16*). Assuming that the proteins encoded by Foxp3-controlled genes contribute to the suppressive activity of T_{reg} cells, it seems likely that further analysis of these pathways will provide insight into T_{reg} mechanisms of action.

In addition to the thymic production of natural $Foxp3^+$ T_{reg} cells, naïve T cells in the periphery acquire Foxp3 expression and T_{reg} function in several experimental settings, including in vitro antigenic stimulation in the presence of transforming growth factor–β (TGF-β) or after chronic antigen stimulation in vivo (*17*, *18*) (Fig. 1). Recent studies indicate that the intestine is a site of $Foxp3^+$ T_{reg} cell development and that specialized intestinal dendritic cells (DCs) promote Foxp3 expression via a mechanism that is dependent on local TGF-β and retinoic acid, a vitamin A metabolite (*19*–*21*). Peripheral development of $Foxp3^+$ T_{reg} cells may therefore represent a mechanism that helps broaden the T_{reg} repertoire in specialized anatomical sites. Recent studies have also revealed a reciprocal relationship between the development of $Foxp3^+$ T_{reg} and effector T cells, so that naïve $CD4^+$ T cells differentiate into $Foxp3^+$ T_{reg} cells in the presence of TGF-β or into T helper 17 (T_H17) cells (which secrete IL-17, a potent proinflammatory cytokine) in the presence of TGF-β and IL-6 (*22*, *23*). Therefore, TGF-β, which can be ubiquitously expressed in tissues, has the paradoxical effect of inducing distinct T cell subsets that appear to have opposing effects on immune responses. Moreover, IL-2 facilitates the differentiation of naïve $CD4^+$ T cells into T_{reg} cells but inhibits their differentiation into T_H17 cells, whereas IL-6 suppresses Foxp3 expression in T_{reg} cells in addition to enhancing T_H17 cell development (*23*, *24*). These results serve to illustrate the complexity of cytokine-mediated control of the differentiation of $Foxp3^+$ T_{reg} cells in the periphery, and further work is required to identify tissue-specific factors that influence the balance between T_{reg} and effector T cells in distinct tissue sites.

Although peripherally induced T_{reg} cells resemble thymically derived T_{reg} cells in phenotype and aspects of their function, future comparative studies of their functional and genetic stability, including the status of chromatin remodeling of the Foxp3 locus, need to be performed with the two populations (*25*). It should also be noted that, in contrast to mouse naïve T cells, in which it is difficult to induce Foxp3 by in vitro T cell receptor (TCR) stimulation, human naïve peripheral blood T cells readily express Foxp3 upon TCR stimulation although the expression level is generally much lower and more transient than in natural T_{reg} cells (*26*). Indeed, it is not yet established whether induced T_{reg} cells have identical functions to those of natural T_{reg} cells, to what extent they contribute to the pool of $Foxp3^+$ T_{reg} cells in the periphery, and whether this activation-induced Foxp3 expression in non-T_{reg} cells serves as a T cell–intrinsic brake on immune responses.

$Foxp3^+$ T_{reg} cells can both directly and indirectly suppress the activation and proliferation of many cell types, including T cells, B cells, DCs, natural killer (NK) cells, and NKT cells in vivo and/or in vitro (*27*, *28*). In vitro suppression of TCR-stimulated proliferation of other T cells is a commonly used assay for assessing T_{reg} cell suppressive activity; however, the mechanisms involved are incompletely understood. A number of different mechanisms have been linked to T_{reg} activity, including cell contact–dependent inhibition of the activation and proliferation of antigen-presenting cells (APCs) and T cells, the killing of either APCs or T cells or both, and suppression via cytokines such as IL-10 and TGF-β (*2*, *27*, *28*). These results suggest that $Foxp3^+$ T_{reg} cells do not suppress

[1]Department of Experimental Pathology, Institute for Frontier Medical Sciences, Kyoto University, Kyoto 606-8507, Japan. [2]Sir William Dunn School of Pathology, University of Oxford, Oxford OX1 3RE, UK.

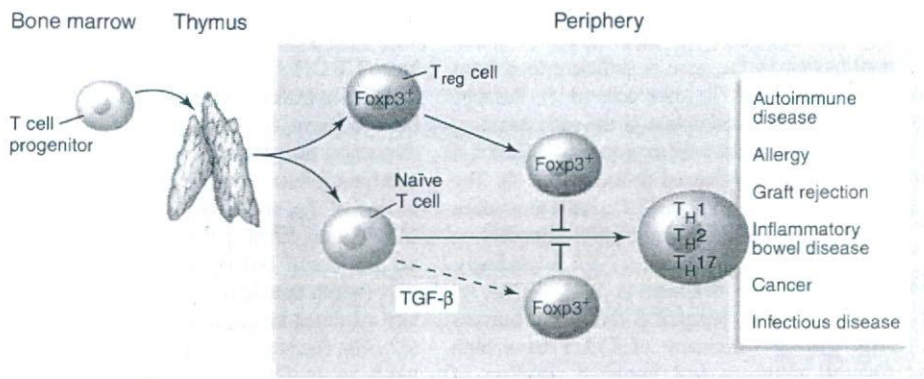

Fig. 1. Foxp3$^+$ natural T_{reg} cells produced by the normal thymus suppress the activation and expansion of naïve T cells and their differentiation to effector T cells, including T_H1, T_H2, and T_H17 cells, which mediate a variety of pathological and physiological immune responses. Foxp3$^+$ T_{reg} cells can also be generated from naïve T cells in the periphery, although the physiological significance of this T_{reg}-generative pathway remains to be determined.

immune responses by a single mechanism but use a variety of pathways in a context-dependent manner; for example, depending on cytokine milieu, the activation status of APCs, and the strength of antigen stimulation. A key challenge therefore is to validate putative mechanisms of T_{reg} activity in vivo and define the circumstances in which these operate. An important factor may be the site of action of T_{reg} cells. Elegant studies by intra-vital imaging with two-photon microscopy to examine the in vivo behavior of activated T_{reg} cells in lymph nodes suggest that they may hamper the access of effector T cells to DCs (*29*, *30*). There is also evidence that T_{reg} cells act in tissues to control established inflammation and that T_{reg} cell production of IL-10 plays a functional role (*2*). IL-10–secreting Foxp3$^+$ T cells are rare in the spleen but abundant in the inflamed intestine and also become detectable at the site of inflammation in autoimmune disease or chronic infection (*31*). This indicates that there is compartmentalization of the T_{reg} response and that mechanisms of suppression may be influenced by the anatomical location and dictated by the nature of the inflammatory response being regulated. It is also imperative to the host that appropriate effector responses can be activated after infection with pathogens. The production of IL-6 by activated DCs has been shown to overcome T_{reg}-mediated suppression in vitro (*32*). However, further information on the cellular and molecular pathways that control the delicate balance between effector and regulatory T cells in vivo is required.

The specialized immunological properties of Foxp3$^+$CD4$^+$ T_{reg} cells suggest that they might be clinically exploited to control a variety of physiological and pathological immune responses (*2*, *10*). These cells can recognize a broad repertoire of self- and nonself-antigens including pathogens (*33*), although their total repertoire is apparently more skewed to recognizing self-antigens (*34*, *35*). Phenotypically they appear in an "antigen-activated" state in the thymus, as illustrated by their high expression levels of various accessory molecules, including adhesion molecules (*10*). Thus, they are poised to exert suppressive function whenever exposed to relevant antigens and thus are suited for controlling autoimmunity. In addition, in contrast to their in vitro hyporesponsiveness to TCR stimulation, many natural T_{reg} cells are in a proliferative state in vivo, presumably as a consequence of the recognition of self-antigens and possibly commensal microbes, and can be stimulated to proliferate by antigenic stimulation (*10*). They are also functionally stable, retaining their suppressive activity after clonal expansion (*10*). By exploiting this stable and robust suppressive activity as well as proliferative capacity, strategies that clonally expand antigen-specific natural T_{reg} cells while inhibiting the activation and expansion of effector T cells may be useful to strengthen or reestablish self-tolerance in autoimmune disease or induce tolerance to nonself-antigens in organ transplantation, allergy, and IBD, or augment feto-maternal tolerance in pregnancy (Fig. 1). As a reciprocal approach, selective reductions in the number or function of natural T_{reg} cells while retaining or enhancing effector T cells may be a strategy for provoking and augmenting tumor immunity in cancer patients or microbial immunity in chronic infection. Biologicals and small molecules with such differential effects on T_{reg} cells and effector T cells may represent a next generation of therapeutic reagents for suppressing or enhancing immune responses with a high level of selectivity (*36*).

Besides Foxp3$^+$ T_{reg} cells, there are a number of Foxp3-nonexpressing T cells with immune suppressive activity that are in the scope of clinical use. These include CD4$^+$ cells producing IL-10 or TGF-β as well as CD8$^+$ T_{reg} cells with different modes of suppression (*28*, *37*). Although the physiological role of these populations in immune homeostasis is not known, they do offer the advantage for clinical use that antigen-specific T_{reg} cells can be prepared relatively easily.

It is now firmly established that Foxp3$^+$ T_{reg} cells, naturally arising or induced, constitute an indispensable component of the immune system. Further elucidation of the molecular and cellular basis of their development and function will facilitate our understanding of immune tolerance and homeostasis and provide ways to better control immune responses for the benefit of the host.

References and Notes

1. S. Sakaguchi, *Cell* **101**, 455 (2000).
2. K. J. Maloy, F. Powrie, *Nat. Immunol.* **2**, 816 (2001).
3. S. Hori, T. Nomura, S. Sakaguchi, *Science* **299**, 1057 (2003).
4. J. D. Fontenot, M. A. Gavin, A. Y. Rudensky, *Nat. Immunol.* **4**, 330 (2003).
5. R. Khattri, T. Cox, S. A. Yasayko, F. Ramsdell, *Nat. Immunol.* **4**, 337 (2003).
6. R. S. Wildin, S. Smyk-Pearson, A. H. Filipovich, *J. Med. Genet.* **39**, 537 (2002).
7. R. Setoguchi, S. Hori, T. Takahashi, S. Sakaguchi, *J. Exp. Med.* **201**, 723 (2005).
8. J. D. Fontenot, J. P. Rasmussen, M. A. Gavin, A. Y. Rudensky, *Nat. Immunol.* **6**, 1142 (2005).
9. L. M. D'Cruz, L. Klein, *Nat. Immunol.* **6**, 1152 (2005).
10. S. Sakaguchi, *Nat. Immunol.* **6**, 345 (2005).
11. Y. Wu *et al.*, *Cell* **126**, 375 (2006).
12. M. Ono *et al.*, *Nature* **446**, 685 (2007).
13. S. F. Ziegler, *Annu. Rev. Immunol.* **24**, 209 (2006).
14. B. S. Cobb *et al.*, *J. Exp. Med.* **203**, 2519 (2006).
15. A. Marson *et al.*, *Nature* **445**, 931 (2007).
16. Y. Zheng *et al.*, *Nature* **445**, 936 (2007).
17. W. Chen *et al.*, *J. Exp. Med.* **198**, 1875 (2003).
18. I. Apostolou, H. von Boehmer, *J. Exp. Med.* **199**, 1401 (2004).
19. D. Mucida *et al.*, *Science* **317**, 256 (2007).
20. C.-M. Sun *et al.*, *J. Exp. Med.*, in press.
21. J. L. Coombes *et al.*, *J. Exp. Med.*, in press.
22. M. Veldhoen *et al.*, *Immunity* **24**, 179 (2006).
23. E. Bettelli *et al.*, *Nature* **441**, 235 (2006).
24. A. Laurence *et al.*, *Immunity* **26**, 371 (2007).
25. S. Floess *et al.*, *PLoS Biol.* **5**, e38 (2007).
26. M. A. Gavin *et al.*, *Proc. Natl. Acad. Sci. U.S.A.* **103**, 6659 (2006).
27. H. Von Boehmer, *Nat. Immunol.* **6**, 338 (2005).
28. E. M. Shevach, *Immunity* **25**, 195 (2006).
29. Q. Tang *et al.*, *Nat. Immunol.* **7**, 83 (2006).
30. C. E. Tadokoro *et al.*, *J. Exp. Med.* **203**, 505 (2006).
31. H. H. Uhlig *et al.*, *J. Immunol.* **177**, 5852 (2006).
32. C. Pasare, R. Medzhidov, *Science* **299**, 1033 (2003).
33. I. J. Suffia *et al.*, *J. Exp. Med.* **203**, 777 (2006).
34. M. S. Jordan *et al.*, *Nat. Immunol.* **2**, 301 (2001).
35. C. S. Hsieh *et al.*, *Nat. Immunol.* **7**, 401 (2006).
36. T. Yamaguchi *et al.*, *Immunity*, in press.
37. M. G. Roncarolo *et al.*, *Immunol. Rev.* **212**, 28 (2006).

38. S.S. is supported by the Japan Science and Technology Agency. F.P. is a Wellcome Trust Senior Fellow in basic biomedical science.

10.1126/science.1142331

Liver International ISSN 1478-3223

BASIC STUDIES

A surgical model of fulminant hepatic failure in rabbits

Kuo-Chen Hung[1,5], Chee-Chien Yong[1], Yaw-Sen Chen[1,5], Hock-Liew Eng[2], Fang-Ying Kuo[2], Chi-Chang Lin[1], Tai-Horng Young[3], Eiji Kobayashi[4], Chao-Long Chen[1] and Chih-Chi Wang[1]

1 Department of Surgery, Chang Gung Memorial Hospital, Kaohsiung Medical Center, Kaohsiung Hsien, Chang Gung University College of Medicine, Taiwan
2 Department of Pathology, Chang Gung Memorial Hospital, Kaohsiung Medical Center, Kaohsiung Hsien, Chang Gung University College of Medicine, Taiwan
3 Institute of Biomedical Engineering, College of Medicine and College of Engineering, National Taiwan University, Taipei, Taiwan
4 Division of Organ Replacement Research and Animal Transgenic Research Center for Molecular Medicine, JiChi Medical School, Tochigi, Japan
5 Department of Surgery, E-Da Hospital and I-Shou University, Kaohsiung, Taiwan

Keywords
animal model – hepatic encephalopathy – intracranial pressure

Abbreviation:
FHF, fulminant hepatic failure; ICP, intracranial pressure; LMI, liver mass index

Correspondence
Chih-Chi Wang, MD, Department of Surgery, Chang Gung Memorial Hospital, Kaohsiung Medical Centre, Chang Gung University College of Medicine, 123, Ta-Pei Road, Niao Sung Hsiang, Kaohsiung Hsien, Taiwan.
Tel: +886 7 7317123, ext: 8093
Fax: 886 7 3790719
e-mail: ufel4996@ms26.hinet.net

Received 22 February 2007
accepted 16 March 2007

DOI:10.1111/j.1478-3231.2007.01512.x

Abstract

Aim: Animal models of fulminant hepatic failure (FHF) have been developed for characterization of disease progression and to evaluate the effectiveness of liver-assist devices, some by treatment with hepatotoxic drugs, viral hepatitis or surgical procedures. We have developed a model in the rabbit by combining resection of the three anterior lobes with ligation of the pedicle of the right lateral lobes, resulting in liver necrosis; the remnant quadrate lobes are left intact. *Materials and methods:* Adult male New Zealand white rabbits ($n = 16$) were used. Six animals were killed to measure the weight of the separate liver lobes. The others ($n = 10$) underwent left neck central line placement to monitor continuous blood pressure and collect blood for laboratory analysis, and a burr hole on the right parietal bone to monitor the intracranial pressure (ICP). Blood laboratory analysis, clinical hepatic encephalopathy and ICP levels were measured in FHF animals ($n = 6$). Animals ($n = 4$) undergoing a sham operation served as controls. *Results:* All FHF animals died between 12 and 26 h after liver surgery from FHF characterized by a progressive increase in liver enzymes, ammonia, total bilirubin, coagulopathy, hepatic encephalopathy and intracranial hypertension. Histological features of the ischaemic lobes showed coagulative necrosis of hepatocytes with absence of nuclei and collapse of cell plates. Brain histology revealed hypoxic cell damage. *Conclusion:* We have developed a simple, reproducible model of FHF in rabbits that has a number of features comparable with clinical FHF patients and is well suited for testing experimental bioartificial liver systems and investigating the pathogenesis of FHF.

Fulminant hepatic failure (FHF) is characterized by rapid onset of encephalopathy following jaundice. FHF is the result of rapid loss of hepatic functions, including metabolic and detoxification functions, precipitated by toxic assault on hepatocytes because of viral hepatitis, idiosyncratic responses or drug overdose. Although liver transplantation is the most accepted mode of treatment for FHF, it is hampered by shortage of donor organs and requires life-long immunosuppression (1). An alternative treatment is needed to bridge the gap until liver transplantation and to allow time for liver regeneration (2). This has led to the development of extracorporeal bioartificial liver devices for short-term support until a suitable organ becomes available (3–5).

The aetiology of FHF is complex and has led to numerous attempts to develop appropriate animal models to help in understanding the pathophysiology of FHF, and to explore various treatment options such as liver cell transplantation or bioartificial liver support (6, 7). Experimentally, FHF can be induced in animals either surgically, through viral hepatitis (8, 9) or by treatment with drugs such as D-galactosamine (10–13) or acetaminophen (14, 15). Both small animals, such as mice and rats (16, 17) and large animals, such as dogs and pigs (15, 16, 18, 19), have been used for laboratory models of FHF. Clinical characteristics, biochemical profiles or histopathological phenotypes are dependent on the method used for inducing FHF. Terblanche and Hickman (20) established the criteria

for an ideal animal model of FHF and stated that an ideal animal model should display reversibility and reproducibility; it should lead to death from liver failure, but also provide a sufficient therapeutic window. Large animal models are preferred, and they should pose minimal hazard to personnel.

Surgical models of FHF have predominantly concentrated on devascularization by portocaval shunt or complete removal of the liver. Such models have biochemical profiles that poorly mimic the clinical conditions observed in humans. Further, these models are reversible only by transplantation and hepatic coma is short lived. Viral hepatitis infection is still a major cause of FHF in some areas of the world. A viral model has been developed recently by using rabbit haemorrhagic disease virus (RHDV) to induce acute liver failure (8, 9); this viral model could fulfil many criteria of a good model for FHF (21). Hepatotoxic drug models include induction of FHF by carbon tetrachloride, D-galactosamine and acetaminophen. These models induce rather well-defined pathological conditions, but they do not reproduce the same histopathological findings as clinical profiles in humans. Induction of FHF by combined hepatectomy and ischaemia in the liver was successfully produced in rats (18).

In order to address biocompatibility and physiologic metabolic function, primary human hepatocytes appear to be the natural choice for cell-based therapy in humans (22). Owing to the shortage of primary human hepatocytes, small- or moderate-scale experimental bioartificial liver systems are needed. We have developed a medium-size animal model to evaluate such systems in rabbits by combining resection of the three anterior liver lobes with ligation of the pedicle of the right lateral lobes; the clinical, biochemical, haemodynamic, intracranial pressure (ICP) and histological features of this model are described. The primary aim of this study was to develop a controlled, surgical model of acute liver failure with complete mortality in rabbits. The medium-size animal model is suitable for testing of a new liver support system. Resection of a large volume of liver and stay of ischaemic liver were relatively mimicking the clinical human setting. The application of liver support system to this animal model will be performed in continuous research.

Materials and methods

Animals

Adult male, New Zealand white (NZW) rabbits, weighing 2.1–2.9 kg, received water and pellet feed *ad libitum* and were kept in cages at 21 °C on a 12-h light/12-h dark cycle. All animal procedures were approved by the Animal Ethics Committee of Chang Gung University, based on guidelines for Laboratory Animal Facilities and Care of Chang Gung University.

The average weight of the liver and its individual lobes, including the three anterior lobes (left lateral, left medial and right medial liver lobes), right lateral lobes and quadrate lobes, were estimated by measuring the livers from six animals. FHF was induced surgically, as described below, in a further six animals and monitored at multiple times (preoperative, 6, 12 and 18 h post-surgery) for blood chemistry, clinical hepatic encephalopathy and ICP. Sham operations were performed on four animals as a control group for comparison.

Surgical procedure

Overnight-fasted animals were anaesthetized by an intramuscular injection of ketamine (50 mg/kg) and Rompum (1 ml/kg, Bayer Leverkusen, Germany). After general anaesthesia, each animal received an intravenous fluid infusion with normal saline (20 ml/kg) via a right ear marginal vein to prevent hypovolaemic status. Body temperature in FHF animals was maintained with lamps and heating pads. Rectal temperature was continuously monitored by an electronic probe (Philips V24E, M1205A, Boston, MA, USA). The sequence of the procedures was central line operation, induction of FHF and then the burr hole procedure.

Central line operation

Central line operation was initiated with a small skin incision on the left of the neck, with care taken to avoid bleeding. The left carotid artery was exposed and cannulated with a catheter (Broviac 4.2Fr, Bard, Salt Lake City, UT, USA) for continuous blood pressure monitoring (Philips) and blood sampling. Next, the left external jugular vein was cannulated and used for the infusion of intravenous fluid and drugs. Hydroxyethyl starch solution (HAES-steril 10%, Fresenius Kabi, Deutschland GmbH, Friedberg, Germany) was infused with 20 ml/kg before the abdominal surgery to prevent hypovolaemic shock owing to liver resection.

Induction of FHF

A midline incision of the abdomen was followed by dissection of the falciform and the left triangular ligament to expose the hepatic vein. The vascular structures and biliary tract (hepatic vein, portal vein, hepatic artery and hepatic duct) to the right lateral liver lobe were ligated. Then, the bilateral medial liver lobes were ligated together and resected, followed by a

Liver International (2007)

similar procedure for the left lateral liver lobe. Special care was taken to fully mobilize the three anterior liver lobes and to place a ligature high around the common pedicle of the left lateral lobe, so that there was no interference with inflow and outflow of the remnant liver lobe (the quadrate lobe) (Fig. 1).

Burr-hole operation

Following the hepatic procedure, a burr hole (3 mm) was drilled over the right parietal skull bone and a dura mater incision (1 mm) was created. Baseline ICP was measured by inserting the tip of a Codman MicroSencor® catheter (Codman MicroSencor, Johnson & Johnson, MA, USA) approximately 3 mm into the parenchyma of the right hemisphere. After initial measurement, the sensor was removed and the scalp wound was dressed with tetracycline ointment and closed with 3-0 nylon sutures.

Clinical monitoring and biochemical measurements

Clinical parameters were monitored postsurgery, including blood pressure and heart rate. Fluid supply with normal saline was maintained at 5 ml/kg/h. In the case of development of hypotension (mean blood pressure < 50 mmHg) or significant elevation of heart rate, fluid resuscitation with normal saline (20 ml/kg) was performed. After recovery from anaesthesia, the behaviour of the animal was monitored regularly. Encephalopathy scoring was adapted from that used by Traber et al. (19) Blood samples were taken prelaparotomy, and at 6, 12 and 18 h after induction of FHF. Arterial blood gas, alanine transaminase (ALT), aspartate transaminase (AST), ammonia, total bilirubin, lactate dehydrogenase (LDH), prothrombin time (PT), sodium and potassium levels were measured using standard techniques. Blood sugar was examined every 4 h using a blood sugar machine (ONE TOUCH Profile, LIFESCAN, CA, USA). Hypoglycaemia was prevented by infusion with 2 ml of 50% glucose/water when the blood sugar level fell below 80 mg/dl. An ICP transducer was used to monitor continuously ICP in surgically treated animals after the development of severe hepatic encephalopathy (19).

A postmortem examination was performed immediately, for analysis of the macroscopic appearance of the abdominal organs and brain. Biopsy specimens of the liver and brain were obtained from each animal and observed under standard H&E staining according to established procedures.

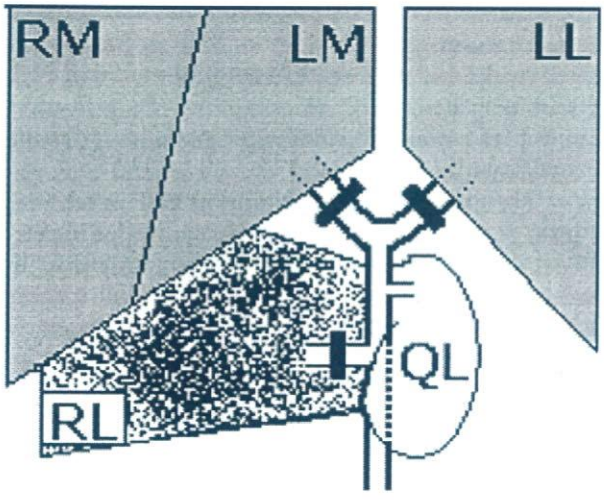

* Resection of 74.28% liver mass (RM + LM + LL).
* Necrosis of 20.15% liver mass (RL).
* Normal residual liver of 5.56% liver mass (QL).

Fig. 1. Diagram depicting the technique used to induce fulminant hepatic failure in rabbits. Resection of the three anterior liver lobes, followed by ligation of the pedicle of the right lateral lobes. RM, right medial lobe; LM, left medial lobe; LL, left lateral lobe; RL, right lateral lobe; QL, quadrate lobe; PV, portal vein.

Statistical analysis

Data are presented as mean $\pm$ SEM. Statistical significance was determined by a *t* test. Correlation was determined by Pearson's product–moment correlation coefficient, *r*. *P* values of ≤ 0.05 were considered to be significant. Statistical analyses were performed using SPSS for Windows version 11.0 (SPSS, Chicago, IL, USA) and EXCEL 2000 (Microsoft).

Results

As a first step, the average liver weight and relative sizes of different liver lobes were estimated using a group of six healthy normal NZW rabbits. All rabbits tolerated the operations well, with minimal intraoperative blood loss. No surgical complications were detected during the period of observation in this study. The operative time of laparotomy, central line placement and burr-hole operation was less than 50 min. Control group animals recovered from anaesthesia about 2 h after surgery and showed no overt paralysis or muscular weakness. In the liver weight and control groups, the three anterior lobes were $74.12 \pm 1.02\%$ of liver mass; the right lateral lobe was $20.22 \pm 0.95\%$; and the quadrate lobe was $5.67 \pm 2.51\%$. The liver mass index (LMI) was the ratio of weight of lobes (g)/body weight (kg). The LMI of three anterior and right lateral lobes was 21.75 ± 1.49 and quadrate lobe, 1.31 ± 0.11. In

FHF animals, the LMI of three anterior and right lateral lobes was 24.30 ± 1.36 ($P = 0.3$) and quadrate lobe, 2.22 ± 0.32 ($P = 0.002$). Correlation between survival and LMI of quadrate lobes was significant ($r = 0.889$).

FHF was induced as described in a set of six animals, and onset of mortality was observed 12–26 h (19.3 ± 2.0) postsurgery (Fig. 2). FHF animals recovered from the anaesthesia 4 h postsurgery but with slow ambulatory motions. This was followed by prostration, impaired balance and side recumbency. Body temperature in FHF rabbits declined, and hence was maintained at 38.5–39.5 °C by passive warming (heating lamp and pads). Increased heart rate (> 270/min) unresponsive to fluid resuscitation and rapid respiration rate with mild distress developed. Consciousness level then decreased markedly with onset of hepatic encephalopathy grade III about 10 h postsurgery. Grade IV hepatic encephalopathy followed, and was short with rapid onset of mortality. Muscular twitching was consistently observed before death.

As shown in Fig. 3, AST, ALT and ammonia levels increased progressively in FHF animals; they remained steady and low in the control group. Hypoglycaemia developed within 6 h postinduction and hence blood sugar was maintained by infusion of dextrose solution. A significant increase in LDH activity and bilirubin as well as prolongation of PT was also observed. While blood electrolyte (Na^+, K^+) levels remained normal, mild acidosis was found in the postoperative period owing to mild CO_2 retention under the effect of anaesthesia. These biochemical studies clearly showed rapid deterioration of liver functions and onset of hepatic injury.

Elevation of ICP ($P < 0.05$ vs. baseline) occurred when hepatic encephalopathy grade III developed and a rapid increase in ICP was observed before death (Fig. 4). Episodic and short increases in ICP, involving sudden elevation, followed by a gradual decline in ICP, were also observed frequently.

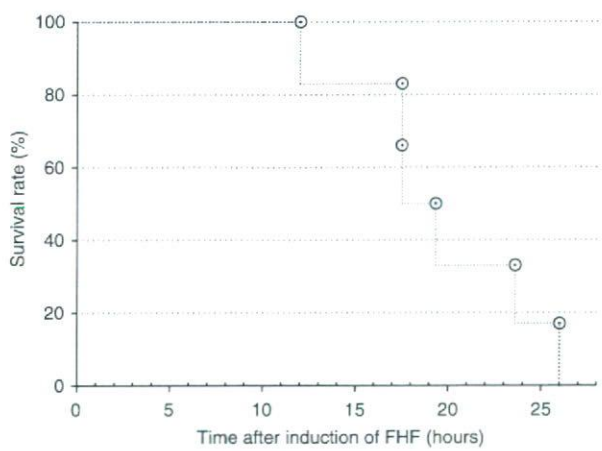

Fig. 2. Survival rate in fulminant hepatic failure animals.

Postmortem examination was performed on all animals to analyse the histopathological complications arising from FHF in this model. In FHF animals, the ischaemic right lateral lobes were scattered with diffuse haemorrhagic spots, while the residual omental lobe showed normal colour. The rest of the abdominal organs were macroscopically normal, with no sign of venous congestion in the spleen, bowel, and the mesentery. No evidence of bleeding around the transducer site or into the subdural space was observed. Under light microscopy, the ischaemic lobe in FHF animals showed focal, lobular coagulative necrosis of haepatocytes with absence of nuclei and collapse of the cell plates (Fig. 5); marked dilatation and congestion of central vein and sinusoids; microvesicular fatty change and dissociation of haepatocytes. Brain biopsy in FHF animals showed nuclear pyknosis of neurons with indistinguishable cytoplasm and neural death scattered over the cortex. Control animals displayed normal histology.

Discussion

FHF in humans is associated with a very high mortality rate and presents as the terminal effect of many types of liver injury. This study is an effort to develop an animal model of FHF for a better understanding of the mechanisms and aetiology of FHF in humans. A novel, stable, and reproducible surgical model of FHF in rabbits is described, which retains many features seen in FHF patients, including progression of hepatic encephalopathy, biochemical alterations and coagulopathy. The major role of this model of FHF in rabbit is to provide the clinician with a more controlled experimental environment that does not ordinarily exist in clinical practice. Although the early surgical models had many high variations in survivals, these more refined resection plus ischaemic models appear to mimic more closely the changes that occur in liver failure. More than with other models, there is no need to perform shunt between portal and systemic veins can be easily reproduced in surgeons.

The need for animal models of FHF is well documented, with numerous attempts using both small and large animals. FHF is usually induced in these animals either by feeding the animals with hepatoxicants such as D-galactosamine (10–13) and acetaminophen (14, 15) or surgically by total liver resection/devascularization (23–26). The drawbacks of hepatoxicant-based FHF induction include poor reproducibility of the model and complications caused

Liver International (2007)

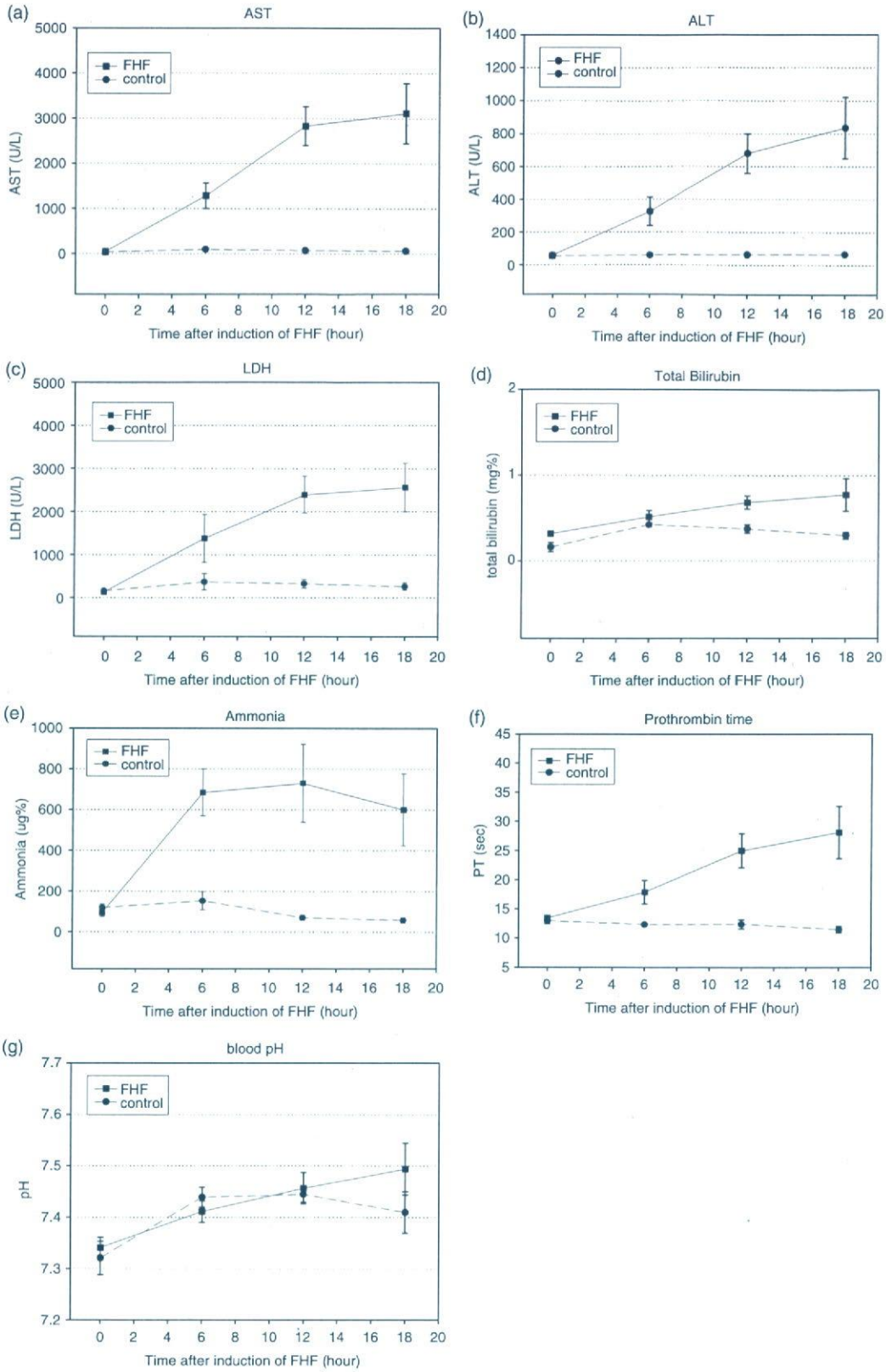

Fig. 3. Time courses of serum levels of aspartate transaminase (a), alanine transaminase (b), lactate dehydrogenase (c), total bilirubin (d), ammonia (e), prothrombin time (f) and pH (g) were measured postsurgery in both fulminant hepatic failure and control animals, indicating marked liver injury and loss of liver function.

by extrahepatic effects of these drugs (e.g. acetaminophen). D-galactosamine-induced FHF is particularly atypical in its clinical manifestation and hence forms a poor model for studying the human disease (20, 26).

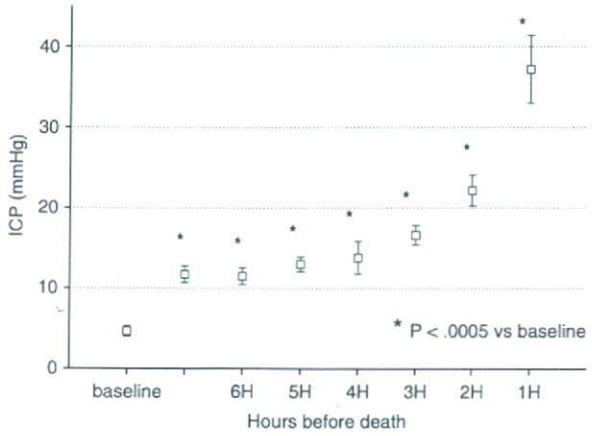

Fig. 4. Intracranial pressure in fulminant hepatic failure animals post surgery.

In viral model, RHDV has been shown to be an adequate animal model for FHF in rabbit. However, the study was limited to rabbit, although it provided minimal risk of transmission to other vertebrate species (27).

Potential disadvantages with existing surgical models based on partial haepatectomy (28, 29), or total haepatectomy (23, 24) are their inability to recreate the inflammatory milieu that exists in acute liver failure. They are accompanied by a stress response that alters the underlying pathophysiological state of liver failure. Furthermore, their relevance as a cause of liver failure in humans such as viral hepatitis and drug-induced hepatotoxicity is rather limited. In this study, we combined the resection of the three anterior lobes (74.12% of the liver) with ligation of the pedicle of the right lateral lobes (20.22% of liver) while the remaining caudate lobes (5.67% of liver) were left intact. This modified version of the previously published procedure in rats (18) is advantageous because it allows for simple surgical induction of FHF displaying various

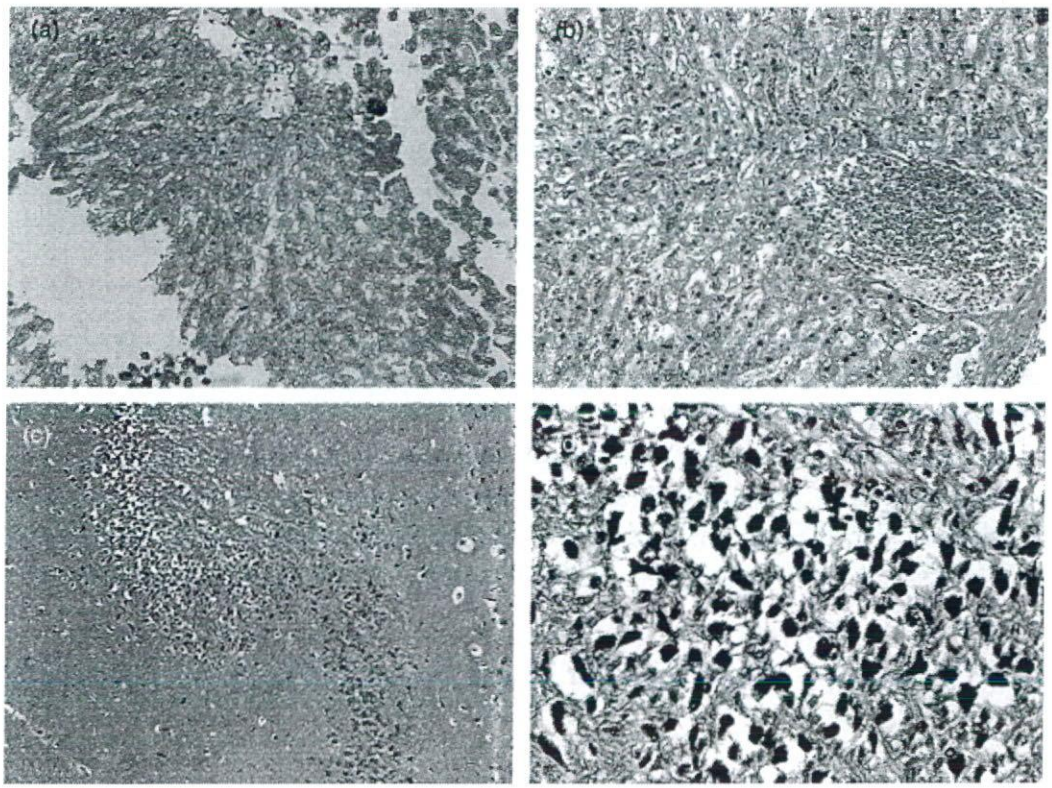

Fig. 5. Histopathological features of: (a) right lateral liver lobe of fulminant hepatic failure (FHF) animals, × 100, hematoxylin and eosin (H&E) staining; focal, lobular coagulative necrosis of hepatocytes with absence of nuclei and collapse of cell plates; (b) right lateral liver lobe of FHF animals, × 100, H&E staining; marked dilatation and congestion of central vein and sinusoids; (c) brain biopsy of FHF animals, × 40, H&E staining; neuronal death in the dentate gyrus of hippocampus; (d) brain biopsy of FHF animals, × 200, H&E staining; cell death in large clusters characterized by nuclear alteration (pyknosis). The nucleus is shrunken and stained darkly. The cytoplasm is indistinguishable.

degrees of severity of disease (based on the amount of native liver left intact in the animal). Ischaemic models of FHF (30, 31) involve complicated surgical procedures, resulting in a greater reliance on surgical expertise (26) and the potential for animal-to-animal variation dependent on the surgeon. Clinical progression of FHF in this surgical model was found to be very similar to that found in human patients, including rapid onset of grade III/IV hepatic encephalopathy, and death between 12 and 26 h postsurgery. Biochemical analysis clearly indicated signs of progressive liver failure and coma, and the animals had a mean survival time of 19.3 h, which may be sufficient for testing support procedures such as treatment with a bioartificial liver. No significant abnormalities in blood electrolytes or blood pH were observed. Histopathological analysis clearly indicated massive hepatic necrosis, and was reflected in elevated plasma levels of AST and ALT.

All animals recovered from anaesthesia and remained haemodynamically stable with continuous infusion of saline. However, decompensated severe hypotension, unresponsive to fluid resuscitation, developed at the end of the experimental period. Arterial O_2 saturation was around 98%. PaO_2 was maintained at more than 100 mmHg in room air.

Brain oedema is a major cause of death in FHF patients (32). The pathogenesis of brain edema and intracranial hypertension in FHF is not clear. Three hypotheses have been proposed: (1) the accumulation of glutamine within astrocytes of the cerebral cortex, (2) products arising from the necrotic liver and (3) abnormalities of the cerebral circulation. The heterogeneous presentation of ICP change in this study implied that multiple factors were involved in the pathogenesis of FHF. ICP was elevated in animals with severe haepticoencephalopathy (19) and we applied the ICP transducer when grade III hepatic encephalopathy developed. Continuous monitoring until death demonstrated elevated ICP in all animals but there were differences in the degree and pattern of ICP changes. The histology of the brain biopsy in FHF animals revealed cell death in large clusters characterized by pyknosis and indistinguishable cytoplasma. It was comparable with hypoxic neuron damage, whereas systemic arterial blood gas did not show low oxygen saturation during the experiment.

In our preliminary study (data not presented), FHF rabbits ($n = 6$) maintained at ambient (21 °C) temperature developed mild hypothermia (32–34 °C) and had a longer survival time (35.5 h) than normothermic FHF animals at 39 °C (19.3 h). It has been reported previously that mild hypothermia has a beneficial effect on uncontrolled brain oedema in FHF (33, 34). One hypothesis for this observation is that hypothermia decreases metabolic demands and reduces the neurotoxicity of ammonia (18).

In the postmortem examination of the FHF animals, there was no significant sign of venous congestion in the spleen, bowel and mesentery, suggesting portal hypertension. There was only a modest (20–22 cmH_2O) increase in portal pressure with acute constriction of the portal vein to $< 20\%$ of the cross-sectional area (18). The mass of the quadrate lobe was statistically different between FHF and control animals (LMI, $P = 0.002$). The increase in residual normal liver weight was caused by oedema (18). Interestingly, there was an association between survival time and LMI of the quadrate lobe ($r = 0.889$). Hence, there is the possibility of a longer survival time due to larger liver mass (oedema) or larger intake liver (not the oedema portion) resulting in extended survival.

The amount of haepatocytes to be loaded in a bioartificial liver for effective support of FHF patients is a fundamental design criterion that has remained unclear. This drawback may have contributed to the inability of many clinical efforts to show efficacy in a statistically significant manner (35). The difficulty in estimating the extent of normal liver function in FHF patients has led to the construction of a standardized BAL therapeutic mode that may not be able to recompense liver functions sufficiently in severely affected patients. These factors have not been studied in detail in most animal models, as developing a reliable FHF model with various degrees of severity has been very difficult. The current surgical procedure, which allows for control of the extent of normal liver function, allows for exactly these kinds of studies. There was $< 10\%$ viable liver mass left in the quadrate lobe. This is a potential reversible model if there is an effective treatment bridging the FHF animal to the stage of sufficient regenerated liver mass. The extent of liver injury should be measurable in an ideal animal model of FHF (18). The residual normal liver function is potentially predicted in this model owing to the advantage of the rabbit liver anatomy, which is separated into five liver lobes.

We have successfully combined two surgical procedures (haepatectomy and ligation of the pedicle of the right lateral lobe), resulting in a reliable, potentially reversible model of FHF in rabbits that displays a number of clinical, biochemical and histological features comparable with clinical FHF patients. This novel medium-size animal model is simple and reproducible and well suited for testing bioartificial liver

support in FHF and the study of more detailed pathophysiology of FHF.

Acknowledgement

The authors thank the National Health Research Institutes of the China for their financial support of project NHRI-EX93-9009EL.

References

1. Bismuth H, Samuel D, Castaing D, Williams R, Pereira SP. Liver transplantation in Europe for patients with acute liver failure. *Semin Liver Dis* 1996; **16**: 415–25.
2. Moreno Gonzalez E, Garcia GI, Loinaz SC, *et al.* Liver transplantation in patients with fulminant hepatic failure. *Br J Surg* 1995; **82**: 118–21.
3. Sauer IM, Zeilinger K, Pless G, *et al.* Extracorporeal liver support based on primary human liver cells and albumin dialysis – treatment of a patient with primary graft non-function. *J Hepatol* 2003; **39**: 649–53.
4. Kreymann B, Seige M, Schweigart U, Kopp KF, Classen M. Albumin dialysis: effective removal of copper in a patient with fulminant Wilson disease and successful bridging to liver transplantation: a new possibility for the elimination of protein-bound toxins. *J Hepatol* 1999; **31**: 1080–5.
5. Rifail K, Ernst T, Kretschmer U, *et al.* Prometheusw – a new extracorporeal system for the treatment of liver failure. *J Hepatol* 2003; **39**: 984–90.
6. Belanger M, Butterworth RF. Acute liver failure: a critical appraisal of available animal models. *Metab Brain Dis* 2005; **20**(4): 409–23.
7. Palmes D, Skawran S, Spiegel HU. Acute liver failure: from bench to bedside. *Transplant Proc* 2005; **37**(3): 1628–31.
8. Tunon MJ, Sanchez-Campos S, Garcia-Ferreras J, Alvarez M, Jorquera F, Gonzalez-Gallego J. Rabbit hemorrhagic viral disease: characterization of a new animal model of fulminant liver failure. *J Lab Clin Med* 2003; **141**(4): 272–8.
9. Sanchez-Campos S, Alvarez M, Culebras JM, Gonzalez-Gallego J, Tunon MJ. Pathogenic molecular mechanisms in an animal model of fulminant hepatic failure: rabbit hemorrhagic viral disease. *J Lab Clin Med* 2004; **144**(4): 215–22.
10. Blitzer BL, Waggoner JG, Jones EA, *et al.* A model of fulminant hepatic failure in the rabbit. *Gastroenterology* 1978; **74**: 664–71.
11. Sielaff TD, Hu MY, Rollins MD, *et al.* An anesthetized model of lethal canine galactosamine fulminant hepatic failure. *Hepatology* 1995; **21**: 796–804.
12. Diaz-Buxo JA, Blumenthal S, Hayes D, Gores P, Gordon B. Galactosamine-induced fulminant hepatic necrosis in unanesthetized canines. *Hepatology* 1997; **25**: 950–7.
13. Nyberg SL. Galactosamine-induced fulminant hepatic failure. *Hepatology* 1997; **26**: 1367–9.
14. Rahman TM, Selden AC, Hodgson HJ. A novel model of acetaminophen induced acute hepatic failure in rabbits. *J Surg Res* 2002; **106**: 264–72.
15. Kelly JH, Koussayer T, He DE, *et al.* An improved model of acetaminophen-induced fulminant hepatic failure in dog. *Hepatology* 1992; **15**: 329–35.
16. Nakama T, Hirono S, Moriuchi A, *et al.* Etoposide prevents apoptosis in mouse liver with D-galactosamine/lipopolysaccharide-induced fulminant hepatic failure resulting in reduction of lethality. *Hepatology* 2001; **33**: 1441–50.
17. Baraldi M, Zeneroli ML, Zanoli P, *et al.* Increased brain concentrations of polyamines in rats with encephalopathy due to a galactosamine-induced fulminant hepatic failure. *Pharmacol Res* 1995; **32**: 57–61.
18. Eguchi S, Kamlot A, Ljubimova J, *et al.* Fulminant hepatic failure in rats: survival and effect on blood chemistry and liver regeneration. *Hepatology* 1996; **24**: 1452–9.
19. Traber PG, Ganger DR, Blei AT. Brain edema in rabbits with galactosamine-induced fulminant hepatitis. *Gastroenterology* 1986; **91**: 1347–56.
20. Terblanche J, Hickman R. Animal models of fulminant hepatic failure. *Dig Dis Sci* 1991; **36**: 770–4.
21. Belanger M, Butterworth RF. Acute liver failure: a critical appraisal of available animal models. *Metab Brain Dis* 2005; **20**(4): 409–23.
22. Tsiaoussis J, Newsome PN, Nelson LJ, Hayes PC, Plevris JN. Which hepatocyte will it be? Hepatocyte choice for bioartificial liver support systems. *Liver Transpl* 2001; **7**: 2–10.
23. Olafsson S, Gottstein J, Blei AT. Brain edema and intracranial hypertension in rats after total hepatectomy. *Gastroenterology* 1995; **108**: 1097–1103.
24. Filipponi F, Boggi U, Meacci L, *et al.* A new technique for total hepatectomy in the pig for testing liver support devices. *Surgery* 1999; **125**: 448–55.
25. Flendrig LM, Calise F, Di Florio E, *et al.* Significantly improved survival time in pigs with complete liver ischemia treated with a novel bioartificial liver. *Int J Artif Org* 1999; **22**: ;701–9.
26. Newsome PN, Plevris JN, Nelson LJ, Hayes PC. Animal models of fulminant hepatic failure: a critical evaluation. *Liver Transpl* 2000; **6**: 21–31.
27. Gould AR, Kattenbelt JA, Lenghaus C, *et al.* The complete nucleotide sequence of rabbit haemorrhagic disease virus (Czech strain V351): use of the polymerase chain reaction to detect replication in Australian vertebrates and analysis of viral population sequence variation. *Virus Res* 1997; **47**(1): 7–17.
28. Demetriou AA, Reisner A, Sanchez A, Levenson SM, Moscioni AD, Chowdhury JR. Transplantation of microcarrier-attached hepatocytes into 90% partial hepatectomized rats. *Hepatology* 1988; **8**: 1006–9.
29. Gaub J, Iversen J. Rat liver regeneration after 90% partial hepatectomy. *Hepatology* 1984; **4**: 902–4.
30. Benoist S, Sarkis R, Baudrimont M, *et al.* A reversible model of acute hepatic failure by temporary hepatic ischemia in the pig. *J Surg Res* 2000; **88**: 63–9.

31. Fourneau I, Pirenne J, Roskams T, Yap SH. An improved model of acute liver failure based on transient ischemia of the liver. *Arch Surg* 2000; **135**: 1183–9.
32. Cordoba J, Blei AT. Brain edema and hepatic encephalopathy. *Semin Liv Dis* 1996; **16**: 271–80.
33. Jalan R, Olde Damink SWM, Lee A, Hayes PC. Moderate hypothermia for uncontrolled intracranial hypertension in acute liver failure. *Lancet* 1999; **354**: 1164–8.
34. Cordoba J, Crespin J, Gottstein J, Blei AT. Mild hypothermia modifies ammonia-induced brain edema in rats after portacaval anastomosis. *Gastroenterology* 1999; **116**: 686–93.
35. Kjaergard LL, Liu J, Als-Nielsen B, Gluud C. Artificial and bioartificial support systems for acute and acute-on-chronic liver failure: a systematic review. *JAMA* 2003; **289**: 217–22.

ORIGINAL ARTICLE

Cytotoxic T-Cell-Mediated Defense Against Infections in Human Liver Transplant Recipients

Koichi Tanaka,[1] Shinji Uemoto,[1] Hiroto Egawa,[1] Yasutsugu Takada,[1] Kazue Ozawa,[2]* Satoshi Teramukai,[3] Mureo Kasahara,[1] Kohei Ogawa,[1] Masako Ono,[2] Hiroshi Sato,[4] Kenji Takai,[5] Masanori Fukushima,[3] and Kayo Inaba[6]

[1]Department of Transplantation and Immunology, Graduate School of Medicine, Kyoto University, Kyoto, [2]Hepatic Disease Research Institute, Kyoto, [3]Division of Clinical Trial Design and Management, Translational Research Center, Kyoto University Hospital, Kyoto, [4]Division of Bioscience, Shiga University of Medical Science, Shiga, [5]Division of Cellular Immunology, SRL Inc., Tokyo, and [6]Division of Systemic Life Science, Graduate School of Medicine, Kyoto University, Kyoto, Japan

Previous studies have shown that postoperative infection is highest in transplant recipients with preexisting high levels of cytotoxic T lymphocytes (CTLs). To study this phenomenon, 106 adult liver transplant recipients were divided into 3 groups, based on hierarchical clustering of the $CD3^+CD8^+CD45$ isoform fractions prior to living donor liver transplantation (LDLT). Group I had the highest naive T-cell levels (subset $CD45RO^-CCR7^+$), Group II had the highest effector/memory (EM) T-cell levels (subset $CD45RO^+CCR7^-$), and Group III had the highest effector T-cell levels (subset $CD45RO^-CCR7^-$). In Group I, CTLs upregulated in response to invading pathogens much earlier and more rapidly than the other groups; this response was associated with $CD4^+$ T-cell help, downregulation of $CD27^+CD28^+$ subsets, and upregulation of interferon-gamma and perforin expression. In contrast, in Groups II and III, CTLs upregulated slowly following persistent viral infection and did not respond efficiently to acute infection. In addition, Group II's cytolytic responses were due mainly to upregulation of the $CD8^+$ EM T-cell fraction, whereas Group III's cytolytic responses were attributable to upregulation of effector T cells. The prevalence of EM or effector T cells was dependent on differentiation of the $CD8^+$ phenotype before LDLT. In conclusion, in most infected transplant recipients who died, generation of $CD8^+$ CTLs had been suppressed without associated $CD4^+$ T-cell help. ***Liver Transpl 13:287-293, 2007.*** © **2007 AASLD.**

Received January 22, 2006; accepted October 23, 2006.

Infectious complications cause significant morbidity and mortality after liver transplantation.[1] We reported previously that in liver transplant recipients undergoing living donor liver transplantation (LDLT), the $CD8^+$ T-cell subpopulation enriched with cytotoxic T lymphocytes (CTLs) is associated with a low survival probability and a high rate of infection.[2] Consistent with the role of effector T cells in cytotoxic effects and the secretion of cytokines within the allograft, $CD8^+$ T cells that are activated preoperatively have a different capacity to generate CTLs, as illustrated by their role in heterologous immunity.[3,4] In particular, the response of a transplant recipient to postoperative infection and alloimmunity depends on the history of previous infections. Accordingly, it would be of interest to determine how modulations of preexisting memory T-cell pools influence the outcome of LDLT.

$CD8^+$ memory T cells contribute to the clearance of alloantigens as well as many viral and bacterial infections after liver transplantation. These CTLs recognize peptide antigens presented by class I molecules encoded within major histocompatibility antigens. The generation of effector responses to infection depends critically on $CD4^+$ helper T cells.[5-7] The chemokine

Abbreviations: LDLT, living donor liver transplantation; CTLs, cytotoxic T lymphocytes; EM, effector/memory T-cell subsets; IL, interleukin; IFN-γ, interferon-gamma; HCV, hepatitis C virus; RNA, ribonucleic acid; HBV, hepatitis B virus.

Supported in part by grants (Nos. 13204041, 13307038, 15390394 and 17390350) from the Scientific Research Fund of the Ministry of Education, Science and Culture, Japan.

Address reprint requests to Kazue Ozawa, Hepatic Disease Research Institute, Honmachi-15 chyome-754-1, Higashiyama-ku, Kyoto, Japan. Telephone: 81-75-561-3005; FAX: 81-75-541-8180; E-mail: kanzou@vesta.ocn.ne.jp

DOI 10.1002/lt.21065
Published online in Wiley InterScience (www.interscience.wiley.com).

receptor CCR7 controls the homing of $CD8^+$ T cells to secondary lymphoid organs. Human memory T cells are divided into 3 functionally distinct subsets according to the distributions of CCR7, CD45RO and perforin: central/memory T cells (subset $CD45RO^+CCR7^+$), effector/memory (EM) T cells (subset $CD45RO^+CCR7^-$) with low levels of perforin, and effector T cells (subset $CD45RO^-CCR7^-$) with high levels of perforin.[8,9] Among the cytokines, the expression of interleukin (IL)-12 and interferon-gamma (IFN-γ) plays an important role in the differentiation and maturation of T cells. IL-12 induces the production of IFN-γ; it favors a cell-mediated response by promoting $CD4^+$EM T-cell differentiation of $CD4^+$ T cells and signaling the expression and differentiation of $CD8^+$ T cells.[10] IL-12 mediates its biological activities by binding to specific cell surface receptors.[11,12] Expression of the costimulatory receptors CD28 and CD27 is also associated with distinct stages of $CD8^+$ T-cell differentiation in association with persistent viral infection in humans.[13] The $CD27^+CD28^+$ T cells undergo transformation to $CD27^-CD28^-$ T cells, which are believed to be fully differentiated T cells that exhibit the greatest cytotoxic activity. These considerations led us to seek to determine the mortality rate due to infections in relation to the degree of $CD8^+$ T-cell cytotoxic activity induced by perforin through upregulated cytokines associated with $CD4^+$ T-cell help after LDLT.

Since tetramer technology is restricted to major histocompatibility-type and antigenic peptides, there are few relevant patients available for study. We sought to clarify the clinical characteristics of clustered recipients with different differentiation phenotypes. We have recently accumulated data indicating that the clinical implications vary for recipients with diverse $CD8^+$ differentiation phenotypes. Accordingly, we used conventional phenotypic analyses for $CD8^+$ and $CD4^+$ T cells. Phenotypic analysis suffices for follow-up to determine clinical inferences and outcomes in longitudinal studies.

PATIENTS AND METHODS

Patients and Allografts

Our study involved 106 subjects who had undergone standard LDLT between 2002 and 2005 at Kyoto University Hospital in Japan. Written informed consent was obtained from each subject before LDLT. The study was approved by the Ethics Committee of Kyoto University Hospital and was conducted in accordance with the 1975 Declaration of Helsinki, as revised in 1996.

Immunosuppression

The initial immunosuppressive regime after LDLT was corticosteroids together with tacrolimus or cyclosporine, according to a standard policy.[2]

Definition and Treatment of Acute Graft Rejection

If clinical and/or laboratory evidence of acute graft rejection occurred, a percutaneous liver biopsy was obtained. Specimens were graded according to the Banff criteria.[14] Rejection was treated according to a standard protocol.[2]

Definition of an Infectious Complication

A bacterial, viral, or fungal infection was assumed to have developed if clinical and/or laboratory evidence consistent with acute infection developed. Such laboratory evidence included relevant positive serologic markers and positive cultures.[15] The criteria for sepsis defined by Bone were applied.[16]

Virology

Serum hepatitis C virus (HCV) ribonucleic acid (RNA) was determined qualitatively by applying the polymerase chain reaction according to a commercially available assay (Amplicor HCV; Roche Molecular Systems, Pleasanton, CA).

Tissue Typing

Serologic tissue typing for human leukocyte antigens A, B (Bw), C, DR and DQ for class I and II loci was undertaken in all patients.

Flow Cytometry

Cell staining was undertaken using monoclonal antibodies as previously reported.[2] Flow cytometry was used to measure cytokine production and intracellular staining for perforin.[2,17] Expression of IL-12 receptors was determined using R-phycoerythrin-conjugated anti-IL-12 receptor beta 1 and IL-12 receptor beta 2 (BD Biosciences, San Diego, CA).

Statistical Analysis

We undertook a hierarchical cluster analysis[18] using JMP 5 (SAS Institute Inc., Cary, NC) to identify clusters of recipients having similar distributions of naïve (subset $CD45RO^-CCR7^+$), central/memory (subset $CD45RO^+CCR7^+$), EM, and effector T cells.[2]

We determined bivariate correlations by applying Spearman rank correlation. Comparisons for continuous variables between groups were undertaken by applying Student's t test and analysis of variance. Comparisons for proportions between groups were undertaken using Fisher exact test. All statistical tests were 2-tailed. Statistical significance was defined as $P < 0.05$.

RESULTS

Hierarchical Clustering According to Preoperative $CD8^+$CD45 Isoform Profiles

A total of 106 adult transplant recipients were divided into 3 groups according to hierarchical clustering based

on pretransplant $CD3^+CD8^+CD45$ isoforms (Table 1). The most abundant pretransplant naive T-cell population occurred in Group I. $CD8^+$ T cells in Group II included the most abundant EM T cells. The most abundant effector T cells occurred in Group III. Accordingly, Groups I, II, and III were designated as naive-, EM- and effector-cell dominant, respectively. In Groups II and III the proportions of cells expressing IFN-γ, tumor-necrosis-factor-alpha and perforin were markedly higher than corresponding proportions in Group I. The proportions of IFN-γ-positive cells were significantly different among Group II and III recipients, but proportions of tumor-necrosis-factor-alpha-positive cells, cells that expressed perforin and IL-12 receptor beta 1^+-positive cells did not differ significantly between these groups. $CD27^+CD28^+$ subsets down-regulated to a similar extent in Groups II and III, but to a greater extent in Groups II and III than in Group I. The proportions of IL-12 receptor beta 1^+ cells were considerably greater in Groups II and III than in Group I. These findings indicate that the $CD8^+$ memory T cells in Groups II and III were already differentiated to a greater extent prior to LDLT than those in Group I.

Characteristics of the recipients, donors, and operations were similar to those reported previously.[2] The median age of recipients was 53 years (range, 19 to 67 years). The median age of donors was 42 years (range, 21 to 64 years). The median time from LDLT to death was 67 days (range, 32 to 351 days).

Table 2 shows the posttransplant infection rates in Groups I, II, and III, as well as in recipients infected with hepatitis B virus (HBV) or HCV and those not infected with HBV or HCV. The diseases of recipients without hepatitis viral infection were biliary atresia (3 cases), primary biliary cirrhosis (14 cases), nonviral fulminant hepatic failure (6 cases), primary sclerosing cholangitis (4 cases), nonviral cirrhosis (6 cases), polycystic disease (2 cases), Caroli's disease (1 case), and Wilson's disease (1 case). One recipient had both HBV and HCV infections and was included in both the HBV- and HCV-infected groups.

Postoperative infection rates increased progressively, from 33.3% in Group I recipients and 42.4% in Group II to 64.9% in Group III recipients. In recipients negative for HBV and HCV, postoperative infection rates were high, but there were no significant differences in the postoperative infection rates among Groups I, II, and III. In contrast, in HBV-positive recipients, the infection rates increased significantly from Group I to III; HCV-positive recipients exhibited similar findings, but the trend was not significant. These findings suggest that the infection rates in HBV- and HCV-negative cases are independent of the $CD8^+$ differentiation phenotype, whereas infection rates in HBV- or HCV-positive cases are strongly dependent on it.

During the study period, 11 (10.4%) of our 106 recipients died. The mortality rate was significantly higher ($P = 0.0190$, chi-square test). Group I vs. Group III was $P = 0.0281$, Group I vs. Group II, $P = 0.6032$, Group II vs. Group III, $P = 0.0898$ (Fisher exact test). Mortality in Group II fell between the rates of the other 2 groups.

TABLE 1. Hierarchical Clustering Into 3 Groups

Group	n	Age (y)	% Naïve T cells	% CM T cells	% EM T cells	% Effector T cells	% $CD27^+CD28^+$ Subsets	% IFN-γ	% TNF-α	% Perforin	% IL-12Rβ1
I	36	47 ± 12	53.91 ± 10.49	7.51 ± 4.06	6.67 ± 5.21	17.72 ± 7.57	70.95 ± 8.72 (27)*	9.82 ± 5.44 (16)	8.52 ± 5.32 (14)	14.15 ± 6.90 (20)	43.10 ± 12.52 (10)
II	33	54 ± 9	19.19 ± 12.53	12.06 ± 5.96	19.62 ± 8.47	26.25 ± 12.40	42.33 ± 16.18 (19)	13.96 ± 8.01 (10)	13.33 ± 7.73 (8)	25.49 ± 10.96 (9)	73.69 ± 12.85 (7)
III	37	52 ± 12	22.45 ± 10.08	5.01 ± 3.17	7.52 ± 4.74	46.96 ± 11.71	43.91 ± 16.76 (22)	25.79 ± 15.97 (8)	24.53 ± 16.53 (7)	31.50 ±13.26 (13)	74.81 ± 11.08 (9)
Variance											
All	P†	0.0278	<0.0001	<0.0001	<0.0001	<0.0001	<0.0001	0.0021	0.0054	<0.0001	<0.0001
I vs. II	P‡	0.0102	<0.0001	0.0004	<0.0001	0.0008	<0.0001	0.1281	0.0991	0.0021	0.0002
I vs. III	P‡	0.0513	<0.0001	0.0048	0.4715	<0.0001	<0.0001	0.0014	0.0032	<0.0001	<0.0001
II vs. III	P‡	0.6290	0.2322	<0.0001	<0.0001	<0.0001	0.7614	0.0567	0.1089	0.2765	0.8552

Abbreviations: CM, central/memory; Rβ1, receptor beta 1; TNF-α, tumor necrosis factor alpha.
NOTE: Values expressed as mean ± SD.
*Numbers of recipients assayed are shown in parentheses.
†*P* values are based on ANOVA.
‡*P* values are based on Student's *t* test.

TABLE 2. Infection Rates in 3 Groups

Group	n	Infection n* (%)	Mortality n† (%)	Nonviral n*	Nonviral Infection n (%)	HBV n*	HBV Infection n (%)	HCV n*	HCV Infection n (%)
Total	106	50 (47.2)	11 (10.4)	37	21 (56.8)	28	11 (39.3)	42	19 (45.2)
I	36	12 (33.3)	1 (2.8)	17 (1)*	8 (47.1)	7	0 (0)	12	4 (33.3)
II	33	14 (42.4)	2 (6.1)	9	6 (66.7)	12† (1)‡	4 (33.3)	13† (1)‡	5 (38.5)
III	37	24 (64.9)	8 (21.6)	11 (2)	7 (63.6)	9 (3)	7 (77.8)	17 (3)	10 (58.8)
Variance									
All	*P*§	0.0211	0.0190		0.6874		0.0058		0.3339
I vs. II	*P*|	0.4363	0.5042		0.6802		0.0856		0.7896
I vs. III	*P*|	0.0071	0.0144		0.3903		0.0019		0.1761
II vs. III	*P*|	0.0599	0.0633		0.7136		0.0436		0.2690

* Parentheses, number of infectious recipients.
†Parentheses, number of deceased recipients.
‡One deceased recipient had HBV and HCV infection.
§*P* value based on chi-square test.
| *P* value based on Fisher exact test.

Differential Responses of $CD8^+$CTLs to Infection

Recipients Who Survived

A Group I recipient (45-year-old male) underwent LDLT for fulminant hepatic failure complicated by severe infection (pneumonia) (Fig. 1). He was infected with methicillin-resistant staphylococcus aureus and other bacteria (gram-positive cocci in catheter, and coagulase negative staphylococci); vancomycin was administered from day 1. For cytomegalovirus infection, detected on day 19, gancyclovir was administered. Trough levels of tacrolimus were low by day 5, but appropriate levels were restored after day 7. The proportions of effector T cells upregulated 12 hours after graft reperfusion; they were maximal at day 5 during severe infection and then decreased as infection abated. These changes in effector T-cell proportions correlated negatively ($r = -0.86$) with naïve T cells, but the proportions of $CD8^+$EM T cells remained unchanged at low levels. When the proportions of effector T cells were maximal, the proportions of cells in the $CD27^+CD28^+$ subset were markedly reduced, and IFN-γ and perforin expression was upregulated. These changes reverted toward normal as infection abated. More importantly, the upregulation of effector T cells correlated positively ($r = 0.91$) with the increase in the proportions of $CD4^+$EM T cells, implying a role for $CD4^+$ T-cell help in the generation of CTLs.

A Group II recipient (67-year-old male) underwent LDLT for HCV-related cirrhosis and hepatocellular carcinoma (Fig. 2). Because of ABO incompatibility, immunosuppressive therapy included, in addition to tacrolimus, administration of methylprednisolone (125 mg/day for the first week and 50 mg/day for the following 2 weeks) and prostaglandin EI (0.01 μg/kg/min for 3 weeks) via the hepatic artery. Cyclophosphamide (100 ng for 30 days) was also administered. Appropriate trough levels of tacrolimus were maintained throughout. Cytomegalovirus infection developed at day 12 and was treated with gancyclovir. A marked upregulation of HCV RNA was apparent at day 26. Both $CD8^+$EM and $CD4^+$EM T-cell proportions increased ($r = 0.78$) from day 2 to 54. By day 61, the proportions of these cells had fallen to preoperative levels and HCV RNA had downregulated. From day 125, severe infection due to Enterobacter cloacae and Enterococcus faecium developed; the infection was associated with high fever (39°C) and C-reactive protein levels (20 mg/L). A granuloma was subsequently found in a liver biopsy obtained at day 170. Tuberculosis was suspected, and levofloxacin, streptomycin, and rifamycin were administered. Despite the severe infection from day 125, the proportions of $CD8^+$EM T cells increased only slightly, and high proportions of $CD4^+$EM T cells changed minimally. These observations suggest that CTLs in EM- or effector-cell-dominant recipients do not respond to infection as rapidly as those in naïve-dominant recipients.

Recipients Who Died

A Group III recipient (56-year-old female) underwent LDLT for HCV-related cirrhosis and hepatocellular carcinoma (Fig. 3). Because of ABO incompatibility, additional immunosuppressive therapy was administered via hepatic artery, as shown in Figure 1. Leakage of bile occurred at day 27, and an intra-abdominal abscess subsequently developed. The patient underwent further surgery at day 57. The patient's condition was seriously compromised by uncontrolled infection with Staphylococcus epidermidis. The proportions of effector T cells, which were 50% greater than prior to LDLT, decreased from day 25 despite the severe infection. Troughs of tacrolimus were maintained at appropriate levels throughout. In association with an increase in HCV RNA, the proportions of effector T cells increased; a maximal—approximately 50%—increase in the proportions of these cells had occurred by about day 90.

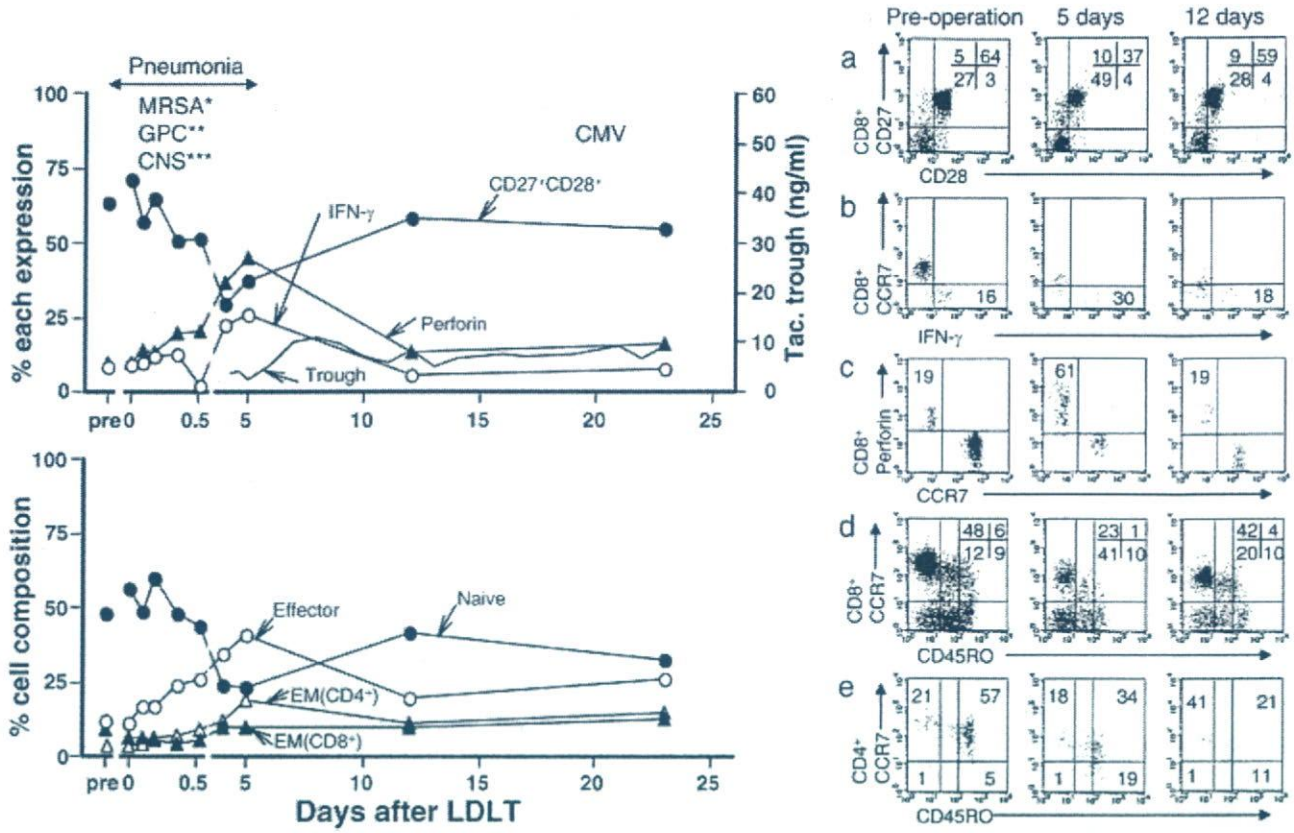

Figure 1. Changes in the proportion of CD8⁺naive, EM, and effector T cells, their cytotoxic activities, and their CD4⁺EM T cell proportion after LDLT in a 45-year-old male (Group I) who underwent LDLT for fulminant hepatic failure. In the left figure, top, perforin and IFN-γ expression are presented as percentages of CD8⁺ T cells. Black circles denotes CD27⁺CD28⁺. Black triangles denote perforin. White circles denote IFN-γ. Irregular line denotes trough. In the left figure, low, black circles denote naïve cells. White circles denote effector cells. White triangles denote EM (CD4⁺). Black triangles denote EM(CD8⁺). In the right figure, flow cytometry, dot plots show double staining for CD27/CD28 (a), CCR7/IFN-γ (b), CCR7/perforin (c), CD8⁺CCR7/CD45RO (d) and CD4⁺CCR7/CD45RO (e) with time defined in days after LDLT. CD28/CD27 cells were gated on CD8⁺ T cells, IFN-γ/CCR7 on CD8⁺CD45RA⁺ cells and CCR7/perforin on CD8⁺CD45RO⁻ cells. The percentages of cells present in quadrants are shown. In the left figure, the proportion of perforin and IFN-γ expression was expressed as a percentage of CD8⁺ T cells. The absolute numbers of effector T cells were expressed as absolute numbers/ul whole blood using white blood cell counts. Pre, pre-LDLT; Tac, tacrolimus; CMV, cytomegalovirus.
***MRSA, Methicillin-resistant staphylococcus in pharynx.**
****GPC, Gram-positive coccus in catheter.**
*****CNS, Coagulase negative staphylococcus in blood culture.**

Thereafter, despite an appreciable increase in HCV RNA, the proportions of effector T cells decreased without upregulation of perforin expression. The proportions of CD4⁺EM T cells remained at low values after LDLT. The proportions of CD8⁺CD27⁺CD28⁺ cells gradually fell from day 50; the decrease was 80% by day 155. The patient died 218 days after the transplant.

DISCUSSION

There is diverse evidence for dynamic changes in CD8⁺ memory T cells before and after LDLT. First, 50 (47.2%) recipients developed infection after LDLT (bacterial in 27.6%, viral in 27.6%, and fungal in 12.1%). Bacterial infections were most frequently caused by Staphylococcus, Enterococcus, or Pseudomonas species. The overall incidence of cytomegalovirus infection after LDLT was 27.6%. There were no serious life-threatening infections with cytomegalovirus.

Second, the incidences of infection after LDLT increased progressively from Group I through Group III recipients; there were no appreciable differences in the incidences of infection between recipients who had HBV-, HCV-, and non-HBV- or non-HCV-related liver disease. Interestingly, the generation of CTLs in response to infection occurred earlier and more rapidly from CD8⁺ naïve-dominant T cells than from CD8⁺EM- or effector-dominant T cells. Effector T cells rapidly upregulated as CD8⁺ naïve T cells downregulated. However, in EM- or effector-cell-dominant recipients the immune responses to infections were less rapid; in these groups there was a gradual response to increasing viremia. This observation suggests that T-cell memory induced by previously encountered pathogens may be modified[19] and may play a crucial role in determining the outcome of infection after LDLT. This inference is consistent with previous immunological exposures to infection resulting in immunological responses that stimulate T-cell memory, which would influence the course of future immunological responses to unrelated

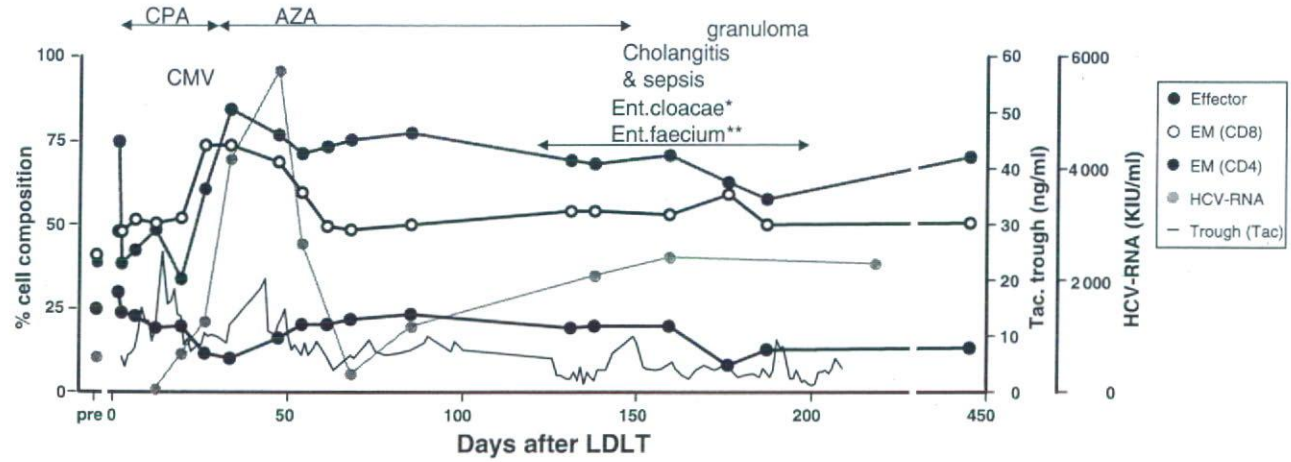

Figure 2. Changes in the proportions of CD8⁺naïve, EM, and effector T cells, their cytotoxic activities, and CD4⁺EM T-cell proportions after LDLT in a 67-year-old male (Group II), who underwent LDLT for HCV-related cirrhosis and hepatocellular carcinoma. Black circles denote effector cells. White circles denote CD8 EM cells. Red circles denote CD4 EM cells. Blue circles denote HCV RNA. Irregular line denotes trough (Tac). Pre, pre-LDLT; Tac, tacrolimus; CPA, cyclophosphamide; AZA, azathioprine; CMV, cytomegalovirus; HCV-RNA, hepatitis C virus-RNA; KIU/ml, kilo international unit/ml.
***Ent. cloacae, enterobacter cloacae in blood and bile culture.**
****Ent. faecium, enterococcus faecium in bile.**

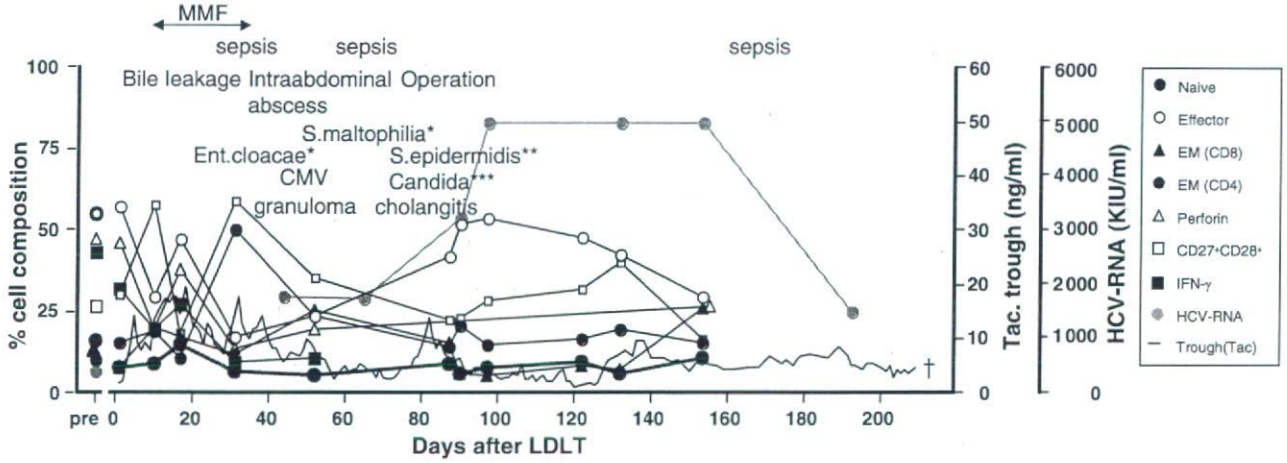

Figure 3. Changes in the proportions of CD8⁺naïve, EM and effector T cells, and CD4⁺EM T cells following severe infection in a Group III recipient who died. A 56-year-old female underwent LDLT for HCV-related cirrhosis and hepatocellular carcinoma, associated with severe sepsis, cytomegalovirus infection, and hyperbilirubinemia. There was donor/recipient ABO incompatibility. Treatment included gancyclovir. She died at day 218. Pre, pre-LDLT; Tac, tacrolimus. Black circles denote naï cells. White circles denote effector cells. Black triangles denote CD8 EM cells. Red circles denote CD4 EM cells. White triangles denote perforin. White boxes denote CD27⁺;CD28⁺. Black squares denote IFN-γ. Blue circles denote HCV RNA. Irregular line denotes trough. Pre, pre-LDLT; Tac, tacrolimus; MMF, mycophenolate mofetil; CMV, cytomegalovirus; HCV-RNA, hepatitis C virus-RNA; KIU/ml, kilo international unit/ml.
***Ent. cloacae, enterobactor cloacae and S. maltophilia, staphylococcus maltophilia in ascites.**
****S. epidermidis, staphylococcus epidermis in blood culture.**
*****Candida in urine.**

pathogens; this phenomenon is known as heterologous immunity.[3] Thus, it would seem likely that the incidences of infection and mortality would be higher in effector-cell-dominant recipients.

Third, in mild infections, the proportions of CTLs increased only slightly, and proportions of CD4⁺EM T cells were almost unchanged. In contrast, in severe infections, CTLs and CD4⁺cell help were significantly upregulated. Of 106 recipients, the frequencies of upregulation of CTLs and CD4⁺ cell help were significantly higher in Group III (83.3%; 10 of 12 infected recipients) than in Group I (57.1%; 4 of 7 infected recipients) or in Group II (62.5%; 5 of 8 infected recipients). Long-term follow-up of large cohorts of recipients is required to determine whether CD4-CD8⁺ cell collaboration develops differentially in the 3 defined groups following infection.

Fourth, the 11 recipients who died exhibited an impaired ability to generate CD4⁺EM T cells. The proportions of CD8⁺EM or effector T cells were not upregulated, and cytotoxicity was suppressed during severe infections in 9 of 11 (81.8%) recipients. With the approach of death, in only 2 recipients (18.2%) did the proportions of